Evolution of the rainfall regime in the United Arab Emirates

T.B.M.J. Ouarda[1, 2*], C. Charron[1], K. Niranjan Kumar[1], P. R. Marpu[1], H. Ghedira[1], A. Molini[1] and I. Khayal[3]

[1] Institute Center for Water and Environment (iWATER), Masdar Institute of Science and Technology, P.O. Box 54224, Abu Dhabi, UAE

[2]INRS-ETE, National Institute of Scientific Research, Quebec City (QC), G1K9A9, Canada

[3]Engineering Systems and Management, Masdar Institute of Science and Technology, P.O. Box 54224, Abu Dhabi, UAE

*Corresponding author:

Email: touarda@masdar.ac.ae

Tel: +971 2 810 9107

To be submitted to Journal of Hydrology

March 2013

Abstract

Arid and semiarid climates occupy more than 1/4 of the land surface of our planet, and are characterized by a strongly intermittent hydrologic regime, posing a major threat to the development of these regions. Despite this fact, a limited number of studies have focused on the climatic dynamics of precipitation in desert environments, assuming the rainfall input – and their temporal trends – as marginal compared with the evaporative component. Rainfall series at four meteorological stations in the United Arab Emirates (UAE) were analyzed for assessment of trends and detection of change points. The considered variables were total annual, seasonal and monthly rainfall; annual, seasonal and monthly maximum rainfall; and the number of rainy days per year, season and month. For the assessment of the significance of trends, the modified Mann-Kendall test and Theil-Sen's test were applied. Results show that most annual series present decreasing trends, although not statistically significant at the 5% level. The analysis of monthly time series reveals strong decreasing trends mainly occurring in February and March. Many trends for these months are statistically significant at the 10% level and some trends are significant at the 5% level. These two months account for most of the total annual rainfall in the UAE. To investigate the presence of sudden changes in rainfall time-series, the cumulative sum method and a Bayesian multiple change point detection procedure were applied to annual rainfall series. Results indicate that a change point happened around 1999 at all stations. Analyses were performed to evaluate the evolution of characteristics before and after 1999. Student's *t*-test and Levene's test were applied to determine if a change in the mean and/or in the variance occurred at the change point. Results show that a decreasing shift in the mean has occurred in the total annual rainfall and the number of rainy days at all four stations, and that the variance has decreased for the total annual rainfall at two stations. Frequency analysis was also performed on data before and after the change point. Results show that rainfall quantile values are significantly lower after 1999. The change point around the year 1999 is linked to various global climate indices. It is observed that the change of phase of the Southern Oscillation Index (SOI) has strong impact over the UAE precipitation. A brief discussion is presented on dynamical basis, the teleconnections connecting the SOI and the change in precipitation regime in the UAE around the year 1999.

Keywords

Rainfall; Arid-climate; Trend; Change-point; Extreme; Seasonality, Teleconnection, Southern Oscillation Index.

1. Introduction

The United Arab Emirates (UAE) is located in the arid southeast part of the Arabian Peninsula. This region is characterized by very scarce and variable rainfall. Without permanent surface water resources, groundwater resources were extensively used for water supply. Recently, strong economic and demographic growth in UAE has put even more stress on water resources. The deficit in water availability between the increasing demand and water resources availability has been met by non-conventional sources such as desalinated water. Groundwater aquifers rely on recharge from rainfall. For this purpose, a large number of small recharge dams were built to capture rainfall water from infrequent but usually intense events. For optimal water resources management, it is important to understand the temporal evolution of rainfall. The main objective of the present study is to analyze rainfall trends in the arid region of the UAE. The variables analyzed in this study are: the total annual, seasonal and monthly rainfall; the annual, seasonal and monthly maximum rainfall, and the number of rainy days per year, season and month.

A relatively limited number of studies dealing with rainfall trend analysis in arid and semi-arid regions have been conducted, with very few dealing with desert environments and the Arabian Peninsula. Modarres and Sarhadi (2009) found that, in Iran, annual rainfall is decreasing at 67% of 145 stations studied while annual maximum rainfall is decreasing at only 50% of the stations. However, only 24 stations exhibit significantly negative trends. Törnros (2010) reported a statistically significant decreasing trend at 5 stations among a total of 37 stations in the southeastern Mediterranean region. Decreasing but non-significant trends in rainfall characteristics were found in the region of Oman by Kwarteng et al. (2009). Gong et al. (2004) observed slightly decreasing trends in rainfall amounts in the semi-arid region of northern China. However, other rainfall characteristics, such as number of rainy days, maximum daily rainfall, precipitation intensity, persistence of daily precipitation and dry spell duration, experienced significant changes.

Hess et al. (1995) found significant decreasing trends in annual rainfalls and in the number of rainy days per year in the arid Northeast part of Nigeria. Neither trends nor abrupt changes in rainfall characteristics were found by Lazaro et al. (2001) at a station located in the semi-arid southeastern part of Spain. Batisani and Yarnal (2010) found significant decreasing trends for rainfall amounts, associated with a decrease in the number of rainy days throughout semi-arid Botswana. In general, most studies conducted in arid or semi-arid regions found decreasing trends in the rainfall regime of these areas. Output of global and regional climate models indicate also an anticipated decrease in rainfall amounts in most arid and semi-arid regions of the globe, although predicted scenarios for arid areas present a high degree of variability (Black et al., 2010; Chenoweth et al., 2011; Hemming et al., 2010).

In this study, a modified version of the original Mann-Kendall (MK) test, to account for serial correlation, was used for the assessment of trends in rainfall time series. The MK test is one of the most commonly used statistical tests for trend detection in hydrological and climatological time series (Türkeş, 1996; Gan, 1998; Fu et al., 2004; Lana et al., 2004; Khaliq et al., 2008, 2009a, 2009b; Modarres and Sarhadi, 2009; Fiala et al., 2010). The main advantage of using a non-parametric statistical test is that it is more suitable for non-normally distributed and censored data, which are frequently encountered in hydrometeorological time series (Yue et al., 2002a). The presence of sudden changes in rainfall time series was also investigated. For this, two methods were used. The first one is the cumulative sums method (Cusum). It is a simple graphical method that allows detecting changes in the mean by identification of linear trends in the plot of the cumulative values of deviations. The second one is a Bayesian multiple change point detection procedure. It can be used to detect changes in the relation of the response variable with explanatory variables. When time is used as explanatory variable, the procedure allows detecting temporal changes in the time-series. Changes in the mean and the variance are also investigated in this study. An analysis and a discussion of the physical causes of any observed changes are also presented in the present work.

The present paper is organized as follows: Section 2 presents the data used in this study. In section 3, the methods used are summarized. Results are presented and discussed in section 4, and conclusions are presented in section 5.

2. Data

The UAE is located in the Southeastern part of the Arabian Peninsula. It is bordered by the Gulf in the north, Oman in the east and Saudi Arabia in the south. It lies approximately between 22°40’N and 26°N and between 51°E and 56°E. The total area of the UAE is about 83600 km^2 and 90% of the land is classified as hot desert. The rest is mainly represented by the mountainous region in the Northeastern part of the country. The climate of the UAE is arid. Rainfall is scarce and shows a high temporal and spatial variability. The mean annual rainfall in the UAE is about 78 mm and ranges from 40 mm in the southern desert region to 160 mm in the northeastern mountains (FAO, 1997).

The data used in this study comes from 4 meteorological stations located in the international airports of the UAE. Total rainfall is recorded on a daily basis. The map in Fig. 1 gives the spatial distribution of the meteorological stations and shows that the western region of the country is not represented in the database. Periods of record range from 30 to 37 years. The station of Ras Al Khaimah is located near the northeastern mountainous region while the Abu Dhabi, Dubai and Sharjah stations are located along the northern coastline.

A list of the rainfall stations as well as basic statistics of the annual rainfall data are given in Table 1. This includes minimum, maximum, mean, standard deviation, coefficient of variation, coefficient of skewness and coefficient of kurtosis. In average, Abu Dhabi receives the smallest amount of rain (63 mm) and Ras Al Khaimah receives the highest amount (127 mm). Minimum total annual rainfall amounts are very low for all stations. The variability of annual rainfall time series is high for all stations with values of the coefficient of variation around one. All skewness values are positive indicating right skewed distributions.

From the daily data, the following variables are computed: total annual and monthly rainfall, annual and monthly maximum daily rainfall, and number of rainy days per year and per month. The number of rainy days is defined here by the number of days per year or per month with an amount of water higher than 0.1 mm. In the present study, the hydrological year starting on September 1st and ending on August 31th has been considered for the computation of annual rainfall series. September 1st has been selected to start the hydrological year because this date is located during a particularly dry period. The use of the calendar year (January 1st to December 31st) would have resulted in splitting the rainy season between two years. Monthly mean values for each variable are presented in Fig. 2. This figure indicates that the majority of the rain falls between December and March for all stations. The figure shows also that the peak of the rainy season occurs earlier (December) in the eastern region and later as we go towards the central region of the UAE. Fig. 3 illustrates the seasonality of rainfall in the UAE through the polar plots of mean monthly maximum rainfalls in the four stations.

3. Methods

3.1. Mann-Kendall test

The non-parametric test of MK (Mann, 1945; Kendall, 1975) was applied to time-series for assessment of trends. For a given data sample $x_1, x_2, ..., x_n$ of size *n*, the MK test statistic *S* is defined by:

$$S = \sum_{i=1}^{n-1} \sum_{j=i+1}^{n} \mathrm{sgn}(x_j - x_i) \quad (1)$$

where x_i and x_j are the data values for periods *i* and *j* respectively and the sgn(x_j - x_i) is the sign function given by:

$$\operatorname{sgn}(x_j - x_i) = \begin{cases} 1 & \text{if} \quad x_j - x_i > 0 \\ 0 & \text{if} \quad x_j - x_i = 0 \\ -1 & \text{if} \quad x_j - x_i < 0 \end{cases} \tag{2}$$

For large values of *n*, the distribution of the *S* statistic can be well approximated by a normal distribution, with mean and variance given respectively by:

$$\mathrm{E}(S) = 0 \tag{3}$$

$$\mathrm{Var}(S) = \frac{n(n-1)(2n+5) - \sum_{i=1}^{m} t_i(i)(i-1)(2i+5)}{18} \tag{4}$$

where *m* is the number of tied values and t_i is the number of ties for the i^{th} tied value. The standardized normal test statistic Z_s is given by:

$$Z_S = \begin{cases} \dfrac{S-1}{\sqrt{\mathrm{Var}(S)}} & \text{if S > 0} \\ 0 & \text{if S = 0} \\ \dfrac{S+1}{\sqrt{\mathrm{Var}(S)}} & \text{if S < 0} \end{cases} \tag{5}$$

A positive value of Z_s indicates an increasing trend while a negative value of Z_s indicates a decreasing trend. The null hypothesis can be rejected at a significance level of *p* if $|Z_s|$ is greater that $Z_{1-p/2}$ where $Z_{1-p/2}$ can be obtained from the standard normal cumulative distribution tables.

To limit the influence of the serial correlation, Hamed and Rao (1998) proposed to modify the variance of the MK statistic *S* to account for autocoerrelation in the data. In this paper, the variance is corrected by considering the lag-1 autocorrelation. The correction of the variance is applied to Z_s only when the sample lag-1 serial correlation coefficient is significant. In this study, the linear trend is removed from the series before computing the effective sample size.

3.2. Cumulative sum method

The cumulative sum (Cusum) method is a graphical approach that is often used for the detection of changes in time series. For a given time series $x_1, x_2, ..., x_n$, the cumulative sum of deviations for any time k is given by:

$$S_k = \sum_{i=1}^{k} (x_i - \bar{x}) \quad (6)$$

Cusum values, given by S_k, are graphically represented as a function of k. Substantial negative or positive slopes indicate sequences of values below or above the mean value. The positions at the intersection of change of slope indicate change points.

3.3. Bayesian multiple change point detection procedure

To detect changes in rainfall time series, the Bayesian multiple change point detection procedure (Seidou and Ouarda, 2007) is used. This technique represents a general procedure to detect the number, magnitudes and positions of multiple change points in the relationship between a set of explanatory variables and a response variable. If no explanatory variables are specified, the procedure detects changes in the time series of the response variable. The response variable is denoted $y_j (j = 1, ..., n)$ or $\mathbf{y}_{\mathrm{nx1}}$ in vectorial form, while $x_{ij} (i = 1, ..., d; j = 1, ..., n)$ represents the j^{th} observation of the i^{th} explanatory variable ($\mathbf{X}_{d^{*}\mathrm{x}n}$ in matrix form). There are n observations and d^{*} explanatory variables. The multiple linear relationship can be represented as:

$$y_j = \sum_{i=1}^{d*} \theta_i x_{ij} + \varepsilon_j, \quad j = 1, ..., n \tag{7}$$

More details about this procedure and the inference of the number and positions of change points are given in Seidou and Ouarda (2007). In this study, we are interested in detecting chronological changes in the time series.

3.4. Frequency analysis

In the present study, fitting of the data is performed in the Matlab environment. For each statistical distribution, a number of efficient fitting methods are considered. A list of "distributions/estimation methods" selected for fitting the data series is presented in Table 2. To evaluate the goodness of fit of the different distributions/methods, the Akaïke information criterion (AIC) (Akaïke, 1970) is used. The model leading to the minimum value of the AIC is the model with the best fit. The AIC is a parsimonious criterion as it takes into consideration the number of estimated parameters in the model following the law of parsimony.

3.5. Student's *t*-test for equality of means

The Student's *t*-test is used to test the null hypothesis H_0 that the means from two samples are equal against the alternative hypothesis H_1 that the means are different. Let $x_{1j}(j = 1, ..., n_1)$ and $x_{2j}(j = 1, ..., n_2)$ be two samples of length n_1 and n_2 with means $\bar{x}_1$ and $\bar{x}_2$ and variances s_1^2 and s_2^2. The Student's test statistic is computed as :

$$t = \frac{\bar{x}_1 - \bar{x}_2}{\sqrt{\frac{s_1^2}{n_1} + \frac{s_2^2}{n_2}}} \qquad (8)$$

The null hypothesis can be rejected at a significance level of p if $|t| \geq t_{1-p/2,\nu}$ where $t_{1-p/2,\nu}$ can be obtained from a *t*-table with ν degrees of freedom.

3.6. Levene's test for equality of variances

The Levene's test (Levene, 1960) is used to test the equality of variances of k samples. For data samples $x_{1j} (j = 1,...,n_1)$ and $x_{2j} (j = 1,...,n_2)$, we define $z_{1j} = |x_{1j} - \tilde{x}_1|$ and $z_{2j} = |x_{2j} - \tilde{x}_2|$ where $\tilde{x}_1$ and $\tilde{x}_2$ are the medians of the first and the second sample respectively. The Levene's test statistic is defined as:

$$W = \frac{(n_1 + n_2 - 2)[n_1(\bar{Z}_1 - Z_{12})^2 + n_2(\bar{Z}_2 - Z_{12})^2]}{\sum_{j=1}^{n_1}(Z_{1j} - \bar{Z}_1)^2 + \sum_{j=1}^{n_2}(Z_{2j} - \bar{Z}_2)^2} \qquad (9)$$

where $\bar{Z}_1 = \frac{1}{n_1}\sum_{j=1}^{n_1} z_{1j}$, $\bar{Z}_2 = \frac{1}{n_2}\sum_{j=1}^{n_2} z_{2j}$ and $Z_{12} = \frac{1}{n_1 n_2}\left(\sum_{j=1}^{n_1} z_{1j} + \sum_{j=1}^{n_2} z_{2j}\right)$. The null hypothesis, that the variances of the two samples are equal, can be rejected at a significance level of p if $|W| \geq F_{1-p/2,1,n_1+n_2-2}$.

3.7. Theil-Sen's slope estimator

The true magnitude of a slope of a given data sample $x_1, x_2, ..., x_n$, can be estimated with the Theil-Sen's estimator (Theil, 1950; Sen, 1968), which is given by:

$$b = \text{median}\left(\frac{x_j - x_i}{j - i}\right) \quad \forall 1 < i < j \qquad (10)$$

where x_i and x_j are the *i*th and *j*th observations. It is a robust estimate of the slope of the trend (Yue et al., 2002b). This method has been recently used to obtain the magnitude of trends in evapotranspiration by Dinpashoh et al. (2011), in temperature by Jhajharia et al. (2013) and in groundwater level and quality by Daneshvar Vousoughi et al. (2013).

4. Results and discussion

Annual time series of all variables for selected stations are presented in Fig. 4. The dotted line represents the linear trend in each series. In the following, only the results given by the modified Mann-Kendall test are presented and commented as they are more reliable in the presence of serial correlation. However, the differences between the results of the classical MK test and the modified MK test are minor. Table 3 presents the results of the modified MK test. It shows the *Z* statistics obtained at each station for each rainfall variable. Statistically significant trends at levels 5% and 10% are identified with the indices *a* and *b* respectively over the corresponding *Z* values.

The *Z* statistics indicate that the majority of annual series have decreasing trends. However, none of these trends are statistically significant. Analysis of the monthly trends reveals that the strongest trends occur during February and March. During these months, all trends are decreasing. Some of the trends are significant at the level of 5% and several are significant at the level of 10%. These trends are important because these two months contribute for most of the total annual rainfall. Several other significant trends occur during July and August for monthly rainfall and maximum rainfalls. Most of the trends are also decreasing during these two months. Some significantly positive trends are also recorded during the month of November.

To further investigate seasonal trends, months have been grouped together into 4 seasons. In addition, the months with the most significant Z statistics, February and March, were grouped together. Again, only the results of the modified Mann-Kendall test are presented and discussed. However, the classical and the modified versions of the MK test led to similar results. Table 3 presents the results of the modified MK test. Winter and summer show decreasing trends, spring shows slightly decreasing trends and autumn shows mixed decreasing and increasing trends. However, not all trends are significant. For Dubai, the total rainfall and the maximum rainfall have a significant decreasing trend at 5% and for Sharjah, the number of rainy days has a significant decreasing trend at a level of 10%. When February and March are grouped together, all trends are decreasing and several trends are significant at the level of 5% and 10%.

Cusum plots are used to investigate the presence of change points in the mean of the time series. For every time series, a change of slope occurs in 1999. Before 1999, slopes are positive and afterwards they become negative until the end of the series.

The Bayesian multiple change point detection procedure was also applied to each annual series as well as the series of the dates of maximum annual rainfall. Fig. 5 illustrates the identified change points and presents the trends for the various segments for the number of rainy days by year series. The results for the other variables lead to identical patterns for all 4 stations and are not presented due to space constraints. It is relevant to mention that the results presented in Fig 5 are for segments with at least 6 years of data, in order to avoid identifying change points that are too close to the edges of the series or for which not enough data is available to justify the conclusions. The Bayesian procedure was also carried out for segments with at least 3, 4 or 5 years of data, and the results were consistent with the ones obtained with segments of 6 years of data.

For most of the series, a shift is detected in 1999 or around this year. Note that given the random nature of the natural variables being analyzed, the exact date of change may not be as important as the existence of the change, the approximate year and the general trends before and after the change. The exact date may be one or two years different from the detected one, depending on the random component for the years neighboring the change. The detected shift confirms the results obtained with the Cusum method. In general, no change in the date of the maximum rainfall is detected. The results of the Bayesian multiple changepoint detection procedure allow for refining our knowledge concerning the evolution of the rainfall regime in the UAE. While the modified MK test results point to a decreasing trend in all variables associated to the rainfall regime, the change point procedure allows us to see that the general trends in these variables are in fact positive throughout the period of record, but with a downward jump around 1999.

Based on these results, it was decided to separate the annual series into two subsamples at the change point year of 1999. The first subsample includes the data from the beginning of each series to 1998 and the second one includes the data from 1999 to the end of each series. The significance of the change in the mean and in the variance in each pair of subsamples is evaluated with the Student's *t*-test and the Levene's test. Results show that there is a shift in the mean of the total annual rainfall and in the mean of the number of rainy days for the four stations. The Levene's test results indicate also a change in the variance of the total annual rainfall for the stations of Abu Dhabi and Dubai.

Fig. 6 presents bar diagrams of the monthly mean values for the total annual rainfall before and after the change in 1999. These diagrams show that, for the months of January, February, March, April and July, most of the stations experienced an important drop in rainfall. The most important drops happened during the months of February and March. For December, rainfall remained about constant for most of the stations. For the other months, rainfall amounts are very low and conclusions cannot be drawn.

True slopes in rainfall variables were investigated with the Theil-Sen's estimator. Table 4 gives the slopes for annual rainfall series and monthly rainfall series for months with significant amount of rainfall before and after the change in 1999. Increasing trends for annual rainfalls, when the samples are divided at the change point, are confirmed with positive slopes for all annual rainfall series.

Fig. 7 presents, in a single polar plot, the annual maximum rainfall for all stations. The blue stars represent the values before the change of 1999 and the red circles indicate the values after the change. Fig. 7 indicates a general decrease in the magnitudes of the maxima for the second portion of the series (after the 1999 change). A shift in the months in which the maxima occurred can also be observed. Indeed, for the first portion of the series, the annual maxima happened generally during the months of February and March, while they happened usually between December and February for the second portion. Fig. 7 confirms that the overall decrease in annual maximum rainfalls observed in all stations after 1999 is also associated to a shift in the timing of these maxima. In general, annual maximum rainfalls seem to be occurring earlier in the winter season during the second segment of the series.

A frequency analysis was also performed on the subsamples of each annual time series for all four stations. All the Distributions/Methods presented in Table 2 were fitted to each subsample (before and after 1999) and, based on the Akaïke criterion, the best Distributions/Methods are selected for each one. Results are presented in Table 5 for the annual total rainfalls, annual maximum rainfalls and number of rainy days. Quantiles corresponding to a number of return periods are presented for each subsample. It can be observed that, for most stations and variables, the values of quantiles drop significantly after the change point. Results presented also include the return periods corresponding to the second subsamples. To compute these return periods, the probabilities corresponding to the quantiles obtained from the first subsample of a given rainfall series are obtained from the distribution and parameters fitted on the second subsample.

For instance, at the Abu Dhabi station, and for annual maximum rainfalls, the value of the quantile corresponding to the T =10 year return period before 1999 is 71 mm. This same value (71 mm) corresponds to a return period of T = 550 years for the second subsample (after 1999). This drastic increase in the return period corresponding to this annual maximum rainfall value clearly illustrates the differences in the rainfall regimes at the Abu Dhabi station before and after 1999.

For the Dubai, Ras Al Khaimah, and Sharjah stations, the return periods corresponding to the 10-year annual maximum rainfall quantile for the first subsample of the series (before 1999) correspond respectively to 135 years, 47 years and 35 years for the second subsample. The differences of the rainfall regimes before and after 1999 at these four stations are so large that a number of return periods cannot be calculated because, often the value of a quantile from the first subsample falls beyond the upper limit of the distribution fitted on the second subsample. This is true for annual total rainfalls, annual maximum rainfalls and number of rainy days per year (Table 5).

However, it is important to put a word of caution. The use of the results presented above has to be done prudently: While it is important to identify trends and jumps in hydro-climatic series, the direct extrapolation of the currently observed trends can be misleading and can convey erroneous results. It is not recommended to extrapolate these results linearly into the future or to extrapolate them for the estimation of quantiles corresponding to large return periods, given the short record length (see Ouarda and El Adlouni, 2011). It is important to carry out the effort of analyzing and understanding the physical mechanisms associated to the inter-annual variability in the rainfall series in the Gulf region.

The analysis of the possible connections between climate oscillation signals and precipitation variability in the UAE is an important step. A number of low frequency climate oscillation indices have been shown to play a role in the success or failure of Indian Monsoon development and to impact hydro-climatic variables in the Indian Ocean region. These include for instance the Southern Oscillation Index (SOI), the Pacific Decadal Oscillation (PDO), the El Niño-Southern Oscillation (ENSO), the East Atlantic (EAO), the Atlantic Multidecadal (AMO), and the Indian Ocean Dipole (IOD) indices (Rasmusson and Carpenter, 1983; Kripalani and Kulkarni, 1997; Kumar et al., 1999, 2006; Krishnamurthy and Goswami, 2000; Ashok et al., 2001; Sahai et al., 2003;

Kripalani et al., 2003; Selvaraju, 2003; Krishnan and Sugi, 2003; Maity and Kumar, 2006; NOAA, 2006).

Fig. 8 illustrates cumulative values of a number of climate indices of potential interest for the Gulf region. The figure indicates that the year 1999 (or somewhere around it) corresponds to a change of phase of these indices. This could explain the shift that was observed in all precipitation variables and in all UAE stations around this year. Correlation values between these low frequency oscillation climate indices and rainfall variables at the six stations of the study are high and reach the value of 0.68.

Nazemosadat et al. (2006) carried out an analysis to detect change-points in precipitation time series in Iran during the 1951-1999 period. They observed a change point in precipitation around 1975 associated with a positive trend during the period after 1975. A strong relationship of precipitation with ENSO events was detected. Nazemosadat et al. (2006) emphasized that precipitation in southern Iran is higher during El Nino periods and weaker during La Nina. Several other authors identified relationships between precipitation and climate oscillation patterns in the Middle East and the ENSO and NAO indices. ENSO was stated to have an influence on climate in southwest Iran (Dezfuli et al., 2010) and Turkey (Karabörk and Kahya, 2003; Karabörk et al., 2005), while NAO was stated to have an influence on meteorological droughts in southwest Iran (Dezfuli et al., 2010), on precipitation and streamflow patterns in Turkey (Kahya, 2011) and on the Middle Eastern climate and streamflow in general (Cullen et al., 2002). The change in precipitation regime in the UAE that is recorded in the present study after 1999 and the fact that this year corresponds also to a change in the SOI phase confirm that ENSO has a strong impact on precipitation in the region. Modarres and Ouarda (2013) reported that the non-linearity and nonstationarity of the SOI volatility have increased in recent decades and that ENSO has become more dynamic and uncertain. This may increase the prediction uncertainty of ENSO-driven climate phenomena.

As cited above, there are several statistical connections between ENSO events and precipitation anomalies around the world. However, it is important to understand how the Sea Surface Temperature (SST) anomalies characteristic of ENSO warm phase (El Niño) and cold phase (La Niña) change the weather patterns over the UAE and the Arabian Peninsula's precipitation. Here, we present a discussion of the teleconnection mechanism that controls the precipitation over the UAE and adjacent regions.

During the ENSO warm phase the air rising at upper levels of the atmosphere eventually diverges. The anomalous divergence and associated vorticity changes in the upper troposphere drive the atmospheric Rossby waves that affect the global atmospheric circulations. The jet streams in the upper troposphere act as wave-guides for the planetary Rossby waves. The anomalous warming in central and eastern Pacific during the ENSO events (warm and cold phase) alters the position of the troughs and ridges of the Rossby waves (e.g., Straus and Shukla, 1997). As an example, we plotted in Figs. 9a & b, the anomalous meridional wind derived from the National Center for Environmental Prediction- Department of Energy (NCEP-DOE) Reanalysis-2 data (Kanamitsu et al., 2002) at 300hPa pressure level (v300hPa) during the winter period (DJFM) of 1997/98 and 2005/06 respectively. The two years happen to coincide with the ENSO warm and cold phase respectively. One can observe the alternating positive and negative v300hPa anomalies in the upper troposphere associated with Rossby waves.

It is also evident from Fig. 9 that there is distinct change of phase of the upper tropospheric Rossby waves during these anomalous winter periods. These large-scale atmospheric teleconnection patterns alter the surface energy balance in extra-tropics, largely due to surface wind speed anomalies affecting sensible and latent heat fluxes (Deser and Blackmon, 1995). This "atmospheric bridge" is expected to operate most effectively during winter when the strong westerly jet streams persistent in the upper troposphere are favorable for the propagation of Rossby waves.

The teleconnection mechanism discussed above shows that ENSO has a strong impact on the UAE precipitation. As discussed previously there exists a change point in the precipitation regime over the UAE around the year 1999. This change should also be reflected in the upper tropospheric flows. In order to see this change point, we have applied the Principal Component Analysis (PCA) to v300hPa anomalies (0^{o}N-60^{o}N) during the winter for the period, 1979-2012. Figs. 10a & b show the time series and spatial pattern of the first principal component (PC1). It is evident from Fig. 10a that there exists inter-annual variability in the PC1 time series with increasing trend from the year 1991. However, the most persistent and consistent trend is observed after 1999.

To strengthen our arguments that SOI causes this change point, the time series of v300hPa PC1 is correlated with detrended global SSTs obtained from Hadley Center (Rayner et al., 2003). Fig. 10c shows the correlation map (at 5% significant level) indicating that the strong link is found in equatorial Pacific SSTs. This supports our previous arguments that the precipitation regime of UAE changes after the year 1999 and linked to the change in SOI phase.

5. Conclusions, discussion and future work

The present work aimed to study the evolution of rainfall climatology in the UAE. Variables analyzed were total annual, seasonal and monthly rainfalls; annual, seasonal and monthly maximum rainfalls; and the number of rainy days per year, season and month. The non-parametric Mann-Kendall test was applied to each time-series. Results show that the annual rainfall series present decreasing trends for all stations although often insignificant. Monthly analysis reveals that the most important trends happen during February and March. For these months, many trends are statistically significant. This is important because these are also the dominant months for rainfalls in the UAE. The Bayesian change point detection procedure and the cumulative sum procedure detected a change point in 1999 for all rainfall series. A frequency analysis was carried out for every rainfall series and for all sites on data before and after this change point. Results indicate an important drop in rainfall characteristics after 1999.

The identification of trends and sudden changes in hydro-climatic time series has been the topic of a large body of literature (for instance Hess et al., 1995; Gong et al., 2004; Kwarteng et al., 2009). While this step represents an important one in the analysis of changes in these series, it is not sufficient to make conclusions concerning the evolution of hydro-climatic regimes and to extrapolate in a prediction (into higher return periods) or forecasting mode (into the future). As indicated in the results section, although significant decreasing trends were identified with the classical and modified MK tests for all variables associated to the rainfall regime, the refinement of the methodology using the change point detection procedure ended up showing that the true signal corresponds in fact to a general increasing trend in these variables throughout the period of record, but with a downward jump around 1999. The change point around the year 1999 is shown to be linked to the change of SOI phase via Rossby wave teleconnections.

Future work can also focus on the application of non-stationary frequency analysis models to rainfall variables in the region (El Adlouni et al., 2007; El Adlouni and Ouarda, 2009). Covariates can be used as explanatory variables for the parameters of these types of models. Another avenue consists in using Empirical Mode Decomposition (EMD) (Lee and Ouarda, 2010, 2011, 2012) to study the historical rainfall characteristics and predict the evolution of these rainfall variables into the future. Future research can also focus on the adaptation of these proposed non-stationary approaches to regional modeling. A limited number of applications have already been presented in this direction (see Leclerc and Ouarda, 2007; or Ribatet et al., 2007) but none of which dealt with arid regions or desert environments. Much work is still required to develop efficient regional frequency analysis models that integrate teleconnections and non-stationary behavior.

Acknowledgment

The authors wish to thank the UAE National Centre of Meteorology and Seismology (NCMS) for having supplied the data used in this study. The authors wish also to thank Drs. O. A. A. Alyazeedi, M. H. Al Tamimi and T. N. Al Hosary from NCMS for their constructive suggestions. The financial support provided by Masdar Institute of Science and Technology is gratefully acknowledged. The authors wish also to thank the Editor, Prof. A. Bardossy, the Associate Editor, Prof. E. Kahya, and two anonymous reviewers whose comments contributed to the improvement of the quality of the paper.

References

Akaike, H., 1970. Statistical predictor for identification. Annals of the Institute of Statistical Mathematics 22, 203-217.

Ashok, K., Guan, Z.Y., Yamagata, T., 2001. Impact of the Indian Ocean Dipole on the relationship between the Indian monsoon rainfall and ENSO. Geophysical Research Letters, 28(23), 4499-4502.

Batisani, N., Yarnal, B., 2010. Rainfall variability and trends in semi-arid Botswana: Implications for climate change adaptation policy. Applied Geography, 30(4), 483-489.

Black, E., Brayshaw, D.J., Rambeau, C.M.C., 2010. Past, present and future precipitation in the Middle East: insights from models and observations. Philos. Trans. R. Soc. A-Math. Phys. Eng. Sci., 368(1931), 5173-5184.

Bobée, B., 1975. The Log Pearson Type 3 Distribution and Its Application in Hydrology. Water Resources Research 11(5), 681-689.

Bobée, B., Ashkar, F., 1988. Sundry averages method (SAM) for estimating parameters of the Log-Pearson Type 3 distribution. Research Report No. 251, INRS-ETE, Quebec City, Canada.

Chenoweth, J. et al., 2011. Impact of climate change on the water resources of the eastern Mediterranean and Middle East region: Modeled 21st century changes and implications. Water Resources Research, 47.

Cullen, H., Kaplan, A., Arkin, P., deMenocal, P., 2002. Impact of the North Atlantic Oscillation on Middle Eastern Climate and Streamflow. Climatic Change, 55(3), 315-338.

Daneshvar Vousoughi, F., Dinpashoh, Y., Aalami, M., Jhajharia, D., 2013. Trend analysis of groundwater using non-parametric methods (case study: Ardabil plain). Stochastic Environmental Research and Risk Assessment, 27(2), 547-559.

Deser, C., and Blackmon, M. L., 1995. On the Relationship between Tropical and North Pacific Sea Surface Temperature Variations. J. Climate, **8**, 1677–1680.

Dezfuli, A., Karamouz, M., Araghinejad, S., 2010. On the relationship of regional meteorological drought with SOI and NAO over southwest Iran. Theoretical and Applied Climatology, 100(1-2), 57-66.

Dinpashoh, Y., Jhajharia, D., Fakheri-Fard, A., Singh, V.P., Kahya, E., 2011. Trends in reference crop evapotranspiration over Iran. Journal of Hydrology, 399(3–4), 422-433.

El Adlouni, S., Ouarda, T.B.J.M., Zhang, X., Roy, R., Bobee, B., 2007. Generalized maximum likelihood estimators for the nonstationary generalized extreme value model. Water Resources Research, 43(3), W03410.

El Adlouni, S., Ouarda, T.B.M.J., 2009. Joint Bayesian model selection and parameter estimation of the generalized extreme value model with covariates using birth-death Markov chain Monte Carlo. Water Resources Research, 45(6), W06403.

FAO, 1997. Irrigation in the near east region in figures. Water report, 9.

Fiala, T., Ouarda, T.B.M.J., Hladný, J., 2010. Evolution of low flows in the Czech Republic. Journal of Hydrology, 393(3–4), 206-218.

Fu, G., Chen, S., Liu, C., Shepard, D., 2004. Hydro-Climatic Trends of the Yellow River Basin for the Last 50 Years. Climatic Change, 65(1), 149-178.

Gan, T.Y., 1998. Hydroclimatic trends and possible climatic warming in the Canadian Prairies. Water Resources Research, 34(11), 3009-3015.

Gong, D.-Y., Shi, P.-J., Wang, J.-A., 2004. Daily precipitation changes in the semi-arid region over northern China. J. Arid. Environ., 59(4), 771-784.

Hamed, K.H., Rao, A.R., 1998. A modified Mann-Kendall trend test for autocorrelated data. Journal of Hydrology, 204(1–4), 182-196.

Hemming, D., Buontempo, C., Burke, E., Collins, M., Kaye, N., 2010. How uncertain are climate model projections of water availability indicators across the Middle East? Philos. Trans. R. Soc. A-Math. Phys. Eng. Sci., 368(1931), 5117-5135.

Hess, T.M., Stephens, W., Maryah, U.M., 1995. Rainfall trends in the north-east arid zone of Nigeria 1961-1990. Agricultural and Forest Meteorology, 74(1-2), 87-97.

Jhajharia, D., Dinpashoh, Y., Kahya, E., Choudhary, R.R., Singh, V.P., 2013. Trends in temperature over Godavari River basin in Southern Peninsular India. International Journal of Climatology, doi:10.1002/joc.3761.

Kahya, E., 2011. The Impacts of NAO on the Hydrology of the Eastern Mediterranean. In: Vicente-Serrano, S.M., Trigo, R.M. (Eds.), Hydrological, Socioeconomic and Ecological Impacts of the North Atlantic Oscillation in the Mediterranean Region. Advances in Global Change Research. Springer Netherlands, pp. 57-71.

Kanamitsu, M., Ebisuzaki, W., Woollen, J., Yang, S. K., Hnilo, J. J., Fiorino, M., and Potter, G., 2002. NCEP-DOE AMIP-II Reanalysis (R-2). Bulletin of the American Meteorological Society, 1631-1643.

Karabörk, M.Ç., Kahya, E., 2003. The teleconnections between the extreme phases of the southern oscillation and precipitation patterns over Turkey. International Journal of Climatology, 23(13), 1607-1625.

Karabörk, M.Ç., Kahya, E., Karaca, M., 2005. The influences of the Southern and North Atlantic Oscillations on climatic surface variables in Turkey. Hydrological Processes, 19(6), 1185-1211.

Kendall, M.G., 1975. Rank Correlation Methods. Griffin, London.

Khaliq, M.N., Ouarda, T.B.M.J., Gachon, P., 2009a. Identification of temporal trends in annual and seasonal low flows occurring in Canadian rivers: The effect of short- and long-term persistence. Journal of Hydrology, 369(1-2), 183-197.

Khaliq, M.N., Ouarda, T.B.M.J., Gachon, P., Sushama, L., 2008. Temporal evolution of low-flow regimes in Canadian rivers. Water Resources Research, 44(8), W08436.

Khaliq, M.N., Ouarda, T.B.M.J., Gachon, P., Sushama, L., St-Hilaire, A., 2009b. Identification of hydrological trends in the presence of serial and cross correlations: A review of selected methods and their application to annual flow regimes of Canadian rivers. Journal of Hydrology, 368(1-4), 117-130.

Kripalani, R.H., Kulkarni, A., 1997. Climatic impact of El Niño/La Niña on the Indian monsoon: A new perspective. Weather, 52(2), 39-46.

Kripalani, R.H., Kulkarni, A., Sabade, S.S., Khandekar, M.L., 2003. Indian monsoon variability in a global warming scenario. Nat. Hazards, 29(2), 189-206.

Krishnamurthy, V., Goswami, B.N., 2000. Indian monsoon-ENSO relationship on interdecadal timescale. Journal of Climate, 13(3), 579-595.

Krishnan, R., Sugi, M., 2003. Pacific decadal oscillation and variability of the Indian summer monsoon rainfall. Climate Dynamics, 21(3-4), 233-242.

Kumar, K.K., Rajagopalan, B., Cane, M.A., 1999. On the Weakening Relationship Between the Indian Monsoon and ENSO. Science, 284(5423), 2156-2159.

Kumar, K.K., Rajagopalan, B., Hoerling, M., Bates, G., Cane, M., 2006. Unraveling the Mystery of Indian Monsoon Failure During El Niño. Science, 314(5796), 115-119.

Kwarteng, A.Y., Dorvlo, A.S., Kumar, G.T.V., 2009. Analysis of a 27-year rainfall data (1977-2003) in the Sultanate of Oman. Int. J. Climatol., 29(4), 605-617.

Lana, X., Martínez, M.D., Serra, C., Burgueño, A., 2004. Spatial and temporal variability of the daily rainfall regime in Catalonia (northeastern Spain), 1950–2000. Int. J. Climatol., 24(5), 613-641.

Lazaro, R., Rodrigo, F.S., Gutierrez, L., Domingo, F., Puigdefabregas, J., 2001. Analysis of a 30-year rainfall record (1967-1997) in semi-arid SE Spain for implications on vegetation. J. Arid. Environ., 48(3), 373-395.

Leclerc, M., Ouarda, T.B.J.M., 2007. Non-stationary regional flood frequency analysis at ungauged sites. Journal of Hydrology, 343(3-4), 254-265.

Lee, T., Ouarda, T.B.M.J., 2010. Long-term prediction of precipitation and hydrologic extremes with nonstationary oscillation processes. Journal of Geophysical Research-Atmospheres, 115.

Lee, T., Ouarda, T.B.M.J., 2011. Prediction of climate nonstationary oscillation processes with empirical mode decomposition. Journal of Geophysical Research-Atmospheres, 116.

Lee, T., Ouarda, T.B.M.J., 2012. Stochastic simulation of nonstationary oscillation hydroclimatic processes using empirical mode decomposition. Water Resources Research, 48.

Levene, H., 1960. Robust Tests for Equality of Variances, Contributions to probability and statistics. Stanford University Press, Stanford, pp. 278-292.

Maity, R., Kumar, D.N., 2006. Bayesian dynamic modeling for monthly Indian summer monsoon rainfall using El Nino-Southern Oscillation (ENSO) and Equatorial Indian Ocean Oscillation (EQUINOO). Journal of Geophysical Research-Atmospheres, 111(D7).

Mann, H.B., 1945. Nonparametric Tests Against Trend. Econometrica, 13(3), 245-259.

Modarres, R., OUARDA, T. B.M.J., 2013. Testing and Modelling the Volatility Change in ENSO, Atmosphere-Ocean, 1-10, 2013, 1–10 http://dx.doi.org/10.1080/07055900.2013.843054.

Modarres, R., Sarhadi, A., 2009. Rainfall trends analysis of Iran in the last half of the twentieth century. Journal of Geophysical Research-Atmospheres, 114.

Nazemosadat, M.J., Samani, N., Barry, D.A., Molaii Niko, M., 2006. ENSO forcing on climate change in Iran: Precipitation analysis. Iranian Journal of Science and Technology, Transaction B: Engineering, 30(B4), 555-565.

NOAA-National Oceanic and Atmospheric Administration, 2006. <http://www.pmel.noaa.gov/tao/elnino/el-nino-story.html>.

Ouarda, T.B.M.J., El-Adlouni, S., 2011. Bayesian Nonstationary Frequency Analysis of Hydrological Variables. Journal of the American Water Resources Association, 47(3), 496-505.

Rasmusson, E.M., Carpenter, T.H., 1983. The relationship between eastern equatorial Pacific sea surface temperature and rainfall over India and Sri Lanka. Mon. Weather Rev. 111, 517–528.

Rayner, N. A., Parker, De. E., Horton, E. B., Folland, C. K., Alexander, J. V., Rowell, D. P., Kent, E. C., and Kaplan, A., 2003. Global analyses of sea surface temperature, sea ice, and night marine air temperature since the late nineteenth century. J. Geophys. Res., 108, 4407, doi:10.1029/2002JD002670, D14.

Ribatet, M., Sauquet, E., Grésillon, J.M., Ouarda, T.B.M.J., 2007. Usefulness of the reversible jump Markov chain Monte Carlo model in regional flood frequency analysis. Water Resources Research, 43(8): W08403.

Sahai, A.K., Pattanaik, D.R., Satyan, V., Grimm, A.M., 2003. Teleconnections in recent time and prediction of Indian summer monsoon rainfall. Meteorology and Atmospheric Physics, 84(3-4): 217-227.

Seidou, O., Ouarda, T.B.M.J., 2007. Recursion-based multiple changepoint detection in multiple linear regression and application to river streamflows. Water Resources Research, 43(7).

Selvaraju, R., 2003. Impact of El Nino-southern oscillation on Indian foodgrain production. Int. J. Climatol., 23(2), 187-206.

Sen, P.K., 1968. Estimates of the Regression Coefficient Based on Kendall's Tau. Journal of the American Statistical Association, 63(324), 1379-1389.

Straus, D. M., and J. Shukla, 1997. Variations of midlatitude transient dynamics associated with ENSO. J. Atmos. Sci., 54, 777-790.

Theil H., 1950. A rank invariant method of linear and polynomial regression analysis, Part 3. Netherlands Akademie van Wettenschappen, Proceedings 53: 1397–1412.

Törnros, T., 2010. Precipitation trends and suitable drought index in the arid/semi-arid southeastern Mediterranean region. In: Servat, E., Demuth, S., Dezetter, A., Daniell, T. (Eds.), Global Change: Facing Risks and Threats to Water Resources. IAHS Publication, pp. 157-163.

Türkeş, M., 1996. Spatial and temporal analysis of annual rainfall variations in Turkey. Int. J. Climatol., 16(9), 1057-1076.

Water Resources Council, Hydrology Committee, 1967. A uniform technique for determining flood flow frequencies. US Water Resour. Counc., Bull. No. 15, Washington, D.C.

Yue, S., Pilon, P., Cavadias, G., 2002a. Power of the Mann-Kendall and Spearman's rho tests for detecting monotonic trends in hydrological series. Journal of Hydrology, 259(1-4), 254-271.

Yue, S., Pilon, P., Phinney, B., Cavadias, G., 2002b. The influence of autocorrelation on the ability to detect trend in hydrological series. Hydrological Processes, 16(9), 1807-1829.

Table 1. Description of rainfall stations and characteristics of total annual rainfall time series. Minimum, maximum, mean, standard deviation (SD), coefficient of variation (C_V), coefficient of skewness (C_S) and coefficient of kurtosis (C_K).

Stations	Latitude	Longitude	Height (m)	Period	Years	Min (mm)	Max (mm)	Mean (mm)	SD (mm)	C_V	C_S	C_K
Abu Dhabi Int'l Airport	24°26	54°39	27	1982-2011	30	0.0	226	63	57	0.9	1.0	3.5
Dubai Int'l Airport	25°15	55°20	8	1975-2011	37	0.3	355	93	77	0.8	1.3	4.9
Ras Al Khaimah Int'l Airport	25°37	55°56	31	1976-2011	36	0.0	461	127	100	0.8	1.3	5.0
Sharjah Int'l Airport	25°20	55°31	34	1981-2011	31	0.2	378	110	92	0.8	1.0	3.8

Table 2. Distributions/Methods fitted to the data.

Distribution	Symbol	Number of parameters	Estimation method
Exponential	EX	2	ML[1], MM[2]
Generalized Pareto	GP	2	MM, WMM[3]
Gumbel	EV1	2	ML, MM, WMM
Inverse Gamma	IG	2	ML
Lognormal	LN2	2	ML
Normal	N	2	ML
Weibull	W2	2	ML, MM
Gamma	G	3	ML, MM
Generalized Gamma	GG3	3	ML, MM
General Extreme Value	GEV	3	ML, MM, WMM
3-Parameters Lognormal	LN3	3	ML, MM
Pearson Type III	P3	3	ML, MM
Log-Pearson Type III	LP3	3	SAM[4], GMM[5], WRC[6]

[1]ML: Maximum Likelihood
[2]MM: Method of Moments
[3]WMM: Weighted Method of Moments
[4]SAM: Sundry Averages Method (Bobée and Ashkar, 1988)
[5]GMM: Generalized Method of Moments (Bobée, 1975)
[6]WRC: Water Research Council (1967)

Table 3. Results of the modified MK test for annual, monthly and seasonal rainfall time series.

Variable	Station	ANN	FEV	MAR	JUL	AUG	NOV	Autumn (Oct-Dec)	Winter (Jan-Mar)	Spring (Apr-Jun)	Summer (Jul-Sept)	Most significant months (Feb-Mar)
Total rainfall	Abu Dhabi	-0.54	-1.94[b]	-1.43	0.49	-1.84[b]	1.92[b]	0.05	-1.36	-1.02	-0.68	-2.66[a]
	Dubai	-0.64	-1.77[b]	-0.99	-1.86[b]	-3.02[a]	1.90[b]	1.02	-1.24	-0.83	-3.16[a]	-2.42[a]
	Ras Al Khaimah	-0.71	-1.10	-1.14	-0.80	-0.71	-0.78	-0.63	-0.47	-0.49	-0.94	-1.41
	Sharjah	-0.59	-0.87	-1.75[b]	-0.20	-0.12	1.52	-0.22	-0.86	-0.83	-0.29	-2.04[a]
Maximum rainfall	Abu Dhabi	0.06	-1.76[b]	-1.46	0.57	-1.87[b]	1.97[a]	0.41	-0.87	-0.84	-0.67	-2.18[a]
	Dubai	-0.50	-1.51	-1.40	-1.84[b]	-3.16[a]	1.88[b]	0.70	-1.40	-0.68	-3.22[a]	-2.56[a]
	Ras Al Khaimah	0.18	-1.03	-1.26	-0.75	-0.75	-0.79	-1.13	-0.36	-0.45	-0.99	-1.25
	Sharjah	-0.36	-0.77	-1.65[b]	-0.22	-0.12	1.54	-0.12	-0.85	-0.70	-0.31	-1.87[b]
Number of rainy days	Abu Dhabi	-0.72	-2.09[a]	-1.89[b]	0.21	-0.48	0.95	0.20	-0.98	-1.12	-0.18	-1.83[b]
	Dubai	0.01	-1.21	-0.90	-0.13	-1.38	2.34[a]	1.13	-0.41	-0.92	-0.91	-1.21
	Ras Al Khaimah	-0.74	-0.71	-1.92[b]	-0.28	-1.17	-0.89	-0.98	-0.74	-0.37	-1.13	-1.53
	Sharjah	-1.13	-1.23	-2.33[a]	-0.76	-1.40	1.02	-0.47	-1.26	-1.87[b]	-1.29	-2.60[a]

[a] trend statistically significant at $p<0.05$.
[b] trend statistically significant at $p<0.1$.

Table 4. Theil-Sen's slopes for annual and monthly rainfall time series before and after the change point in 1999.

Variable	Station	Before 1999						After 1999					
		ANN	DEC	JAN	FEV	MAR	APR	ANN	DEC	JAN	FEV	MAR	APR
Total rainfall	Abu Dhabi	5.75	0.00	1.69	-0.44	-0.01	-0.05	3.85	0.00	0.43	0.00	0.00	0.01
	Dubai	4.87	0.06	0.71	-0.34	0.65	-0.12	6.65	0.00	0.61	0.02	-0.01	0.09
	Ras Al Khaimah	6.08	0.41	2.16	0.00	0.80	0.01	8.64	0.00	1.07	0.23	0.00	0.00
	Sharjah	10.14	0.05	2.44	0.00	-0.05	0.01	9.88	0.26	0.48	0.15	0.00	0.02
Maximum rainfall	Abu Dhabi	1.47	0.00	0.78	-0.35	0.00	-0.04	1.64	0.00	0.18	0.00	0.00	0.00
	Dubai	0.75	0.05	0.42	-0.05	0.25	-0.07	1.01	0.00	0.42	0.02	-0.04	0.08
	Ras Al Khaimah	1.57	0.32	0.99	0.00	0.56	0.01	0.69	0.00	0.68	0.11	0.04	0.00
	Sharjah	1.22	0.05	1.11	0.00	0.05	0.02	0.90	0.14	0.38	0.12	0.00	0.04
Number of rainy days	Abu Dhabi	1.00	0.00	0.30	0.00	0.00	-0.03	0.72	0.00	0.33	0.00	0.00	0.00
	Dubai	0.62	0.05	0.13	0.00	0.15	0.00	0.78	0.00	0.20	0.11	0.00	0.13
	Ras Al Khaimah	0.50	0.00	0.11	0.00	0.13	0.00	1.00	0.06	0.27	0.14	0.00	0.00
	Sharjah	0.69	0.00	0.30	0.00	0.00	0.00	1.00	0.00	0.19	0.00	0.00	0.00

Table 5. Quantiles (*Q*) of annual total rainfalls (mm), annual maximum rainfalls (mm) and the number of rainy days by year with distributions fitted to data before and after 1999. Return periods indicated as "*T* after 1999" are the return periods of the rainfall "Q before 1999" if evaluated with the distribution corresponding to rainfall after 1999.

Variable	*T* before 1999	Abu Dhabi *Q* before 1999	Abu Dhabi *Q* after 1999	Abu Dhabi *T* after 1999	Dubai *Q* before 1999	Dubai *Q* after 1999	Dubai *T* after 1999	Ras Al Khaimah *Q* before 1999	Ras Al Khaimah *Q* after 1999	Ras Al Khaimah *T* after 1999	Sharjah *Q* before 1999	Sharjah *Q* after 1999	Sharjah *T* after 1999
Total rainfall	2	72	22	7	98	47	8	135	71	5	128	57	6
	5	141	59	33	180	86	*	236	140	*	240	117	*
	10	180	89	77	232	104	*	300	169	*	295	142	*
	20	209	119	149	280	116	*	357	187	*	335	155	*
	50	238	160	280	339	126	*	427	199	*	369	164	*
	100	254	191	397	381	131	*	475	205	*	386	168	*
Maximum rainfall	2	21	14	3	32	21	4	34	26	3	39	20	4
	5	50	29	28	60	36	30	56	47	9	69	43	17
	10	71	38	550	80	46	135	68	57	47	83	59	35
	20	91	46	*	99	55	584	79	63	*	92	73	60
	50	119	55	*	123	67	3863	92	69	*	99	89	95
	100	139	60	*	142	76	15717	101	71	*	102	100	117
Number of rainy days	2	14	7	6	15	9	5	19	12	6	18	10	5
	5	21	13	*	23	16	15	26	18	47	24	18	26
	10	25	15	*	27	20	33	30	21	200	27	21	*
	20	29	17	*	31	24	66	33	23	809	29	24	*
	50	34	18	*	35	29	157	36	26	4846	32	25	*
	100	37	19	*	38	33	290	38	28	18131	34	26	*

* the upper limit of the distribution has been reached.
The units of Q are (mm) for the variables "Total rainfall" and "Maximum rainfall", and (number of days) for the variable "Number of rainy days".

Figure Captions

Fig. 1. Spatial distribution of the meteorological stations.

Fig. 2. a) Mean total monthly rainfalls, b) mean monthly maximum rainfalls and c) mean number of rainy days by month.

Fig. 3. Mean monthly maximum rainfalls on polar plot for each station.

Fig. 4. Annual time series of all variables for selected stations.

Fig. 5. Detection of trend changes for the number of rainy days by year at each station.

Fig. 6. Bar graphs of mean total monthly rainfalls for each station.

Fig. 7. Polar plot of the annual maximum rainfall for all stations.

Fig. 8. Climate oscillation indices of potential interest for the Gulf region.

Fig. 9. The seasonal mean (DJFM) meridional wind anomaly at 300hPa pressure level obtained from NCEP-DOE Reanalysis-2 for the years (a) 1997/98 and (b) 2005/06.

Fig 10. (a) Time series of PC1 of v300hPa anomaly for the winter period (DJFM) (b) Spatial pattern of v300hPa PC1 and (c) Correlation map of v300hPa PC1 and detrended global SSTs for the period 1979-2012.

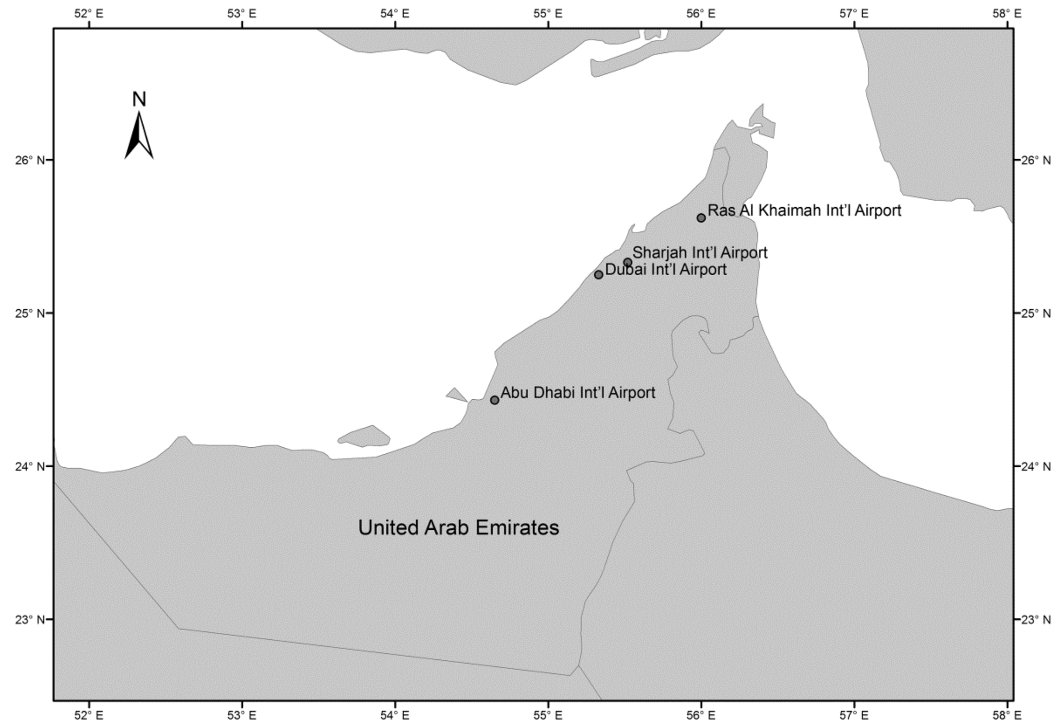
52° E
53° E
54° E
55° E
56° E
57° E
58° E
26° N
25° N
24° N
23° N
N
Ras Al Khaimah Int'l Airport
Sharjah Int'l Airport
Dubai Int'l Airport
Abu Dhabi Int'l Airport
United Arab Emirates

Figure 1.

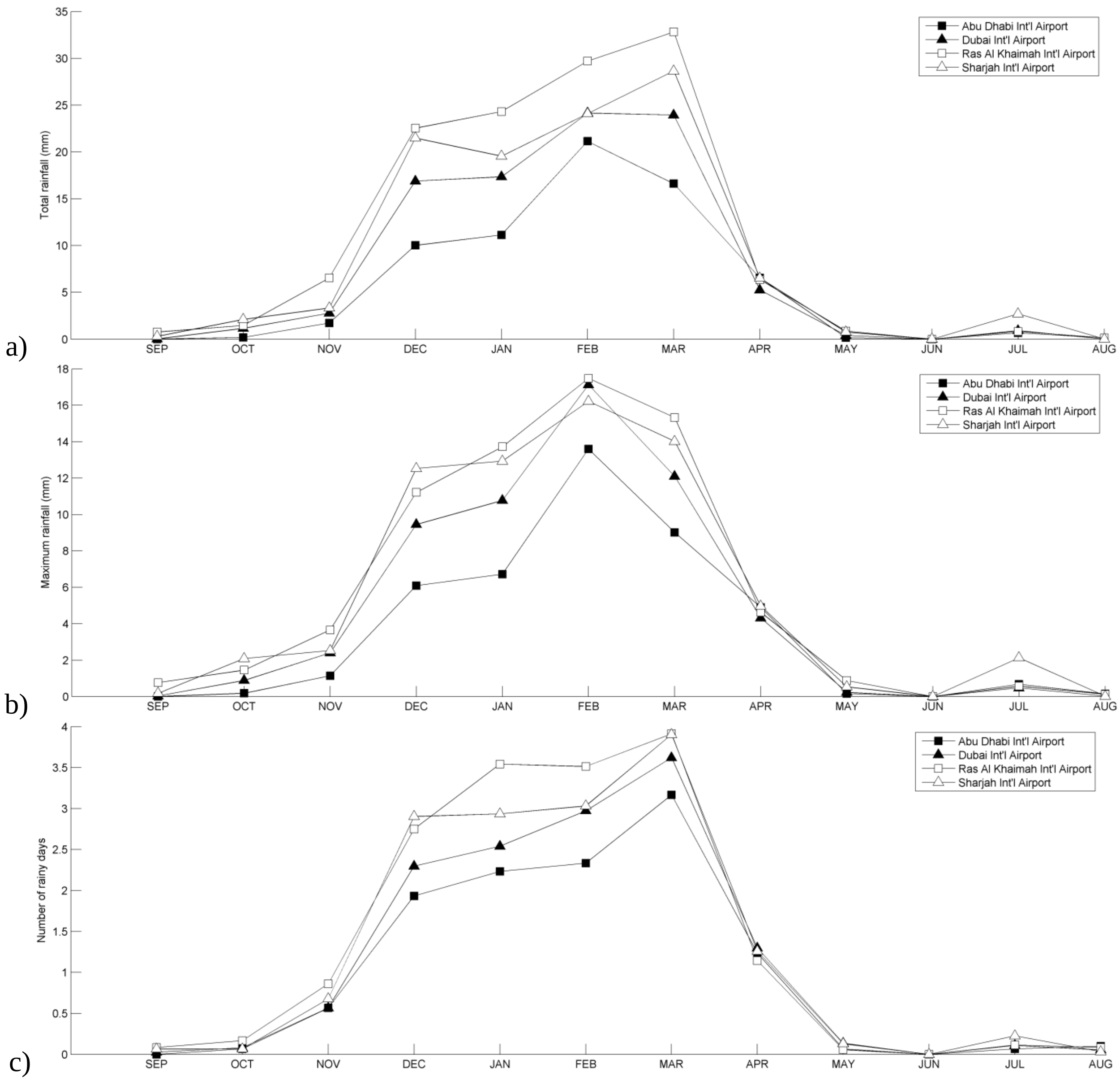
a)
Total rainfall (mm)
Abu Dhabi Int'l Airport
Dubai Int'l Airport
Ras Al Khaimah Int'l Airport
Sharjah Int'l Airport
SEP OCT NOV DEC JAN FEB MAR APR MAY JUN JUL AUG
b)
Maximum rainfall (mm)
c)
Number of rainy days

Figure 2.

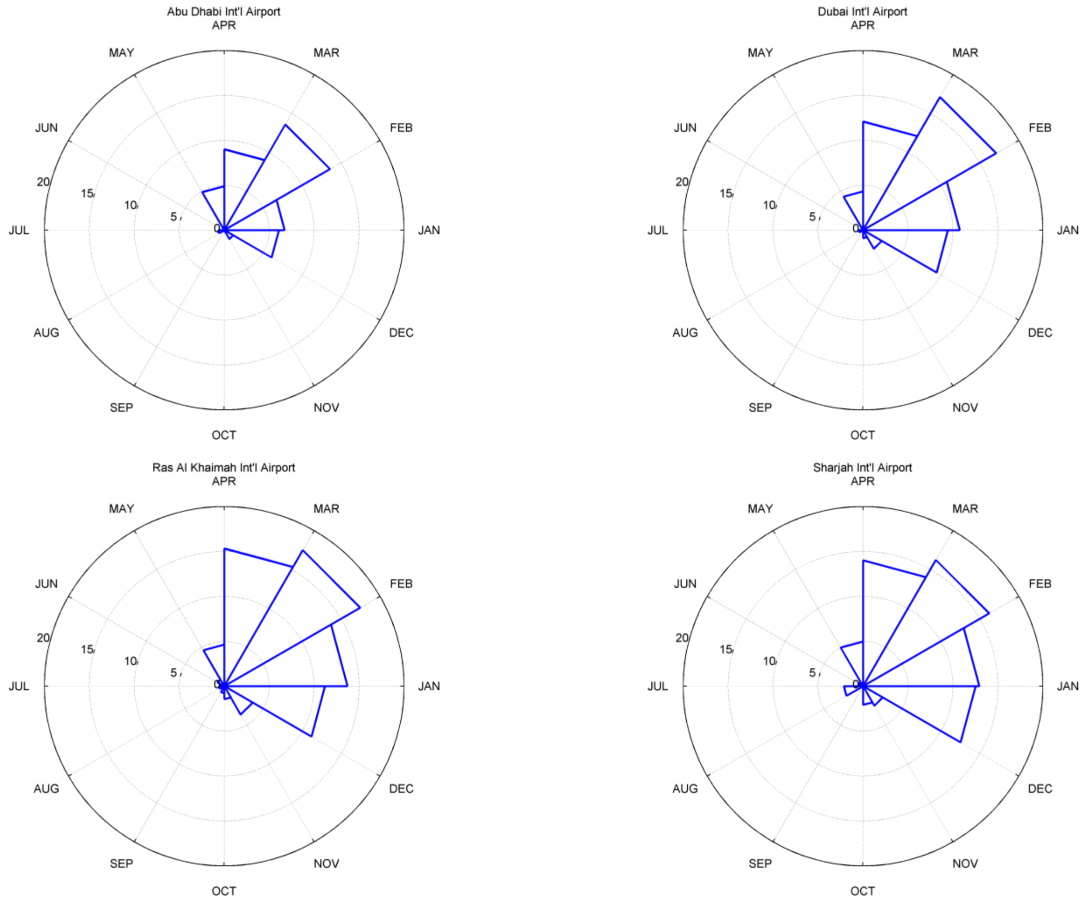
Abu Dhabi Int'l Airport
Dubai Int'l Airport
Ras Al Khaimah Int'l Airport
Sharjah Int'l Airport
JAN
FEB
MAR
APR
MAY
JUN
JUL
AUG
SEP
OCT
NOV
DEC
0
5
10
15
20

Figure 3.

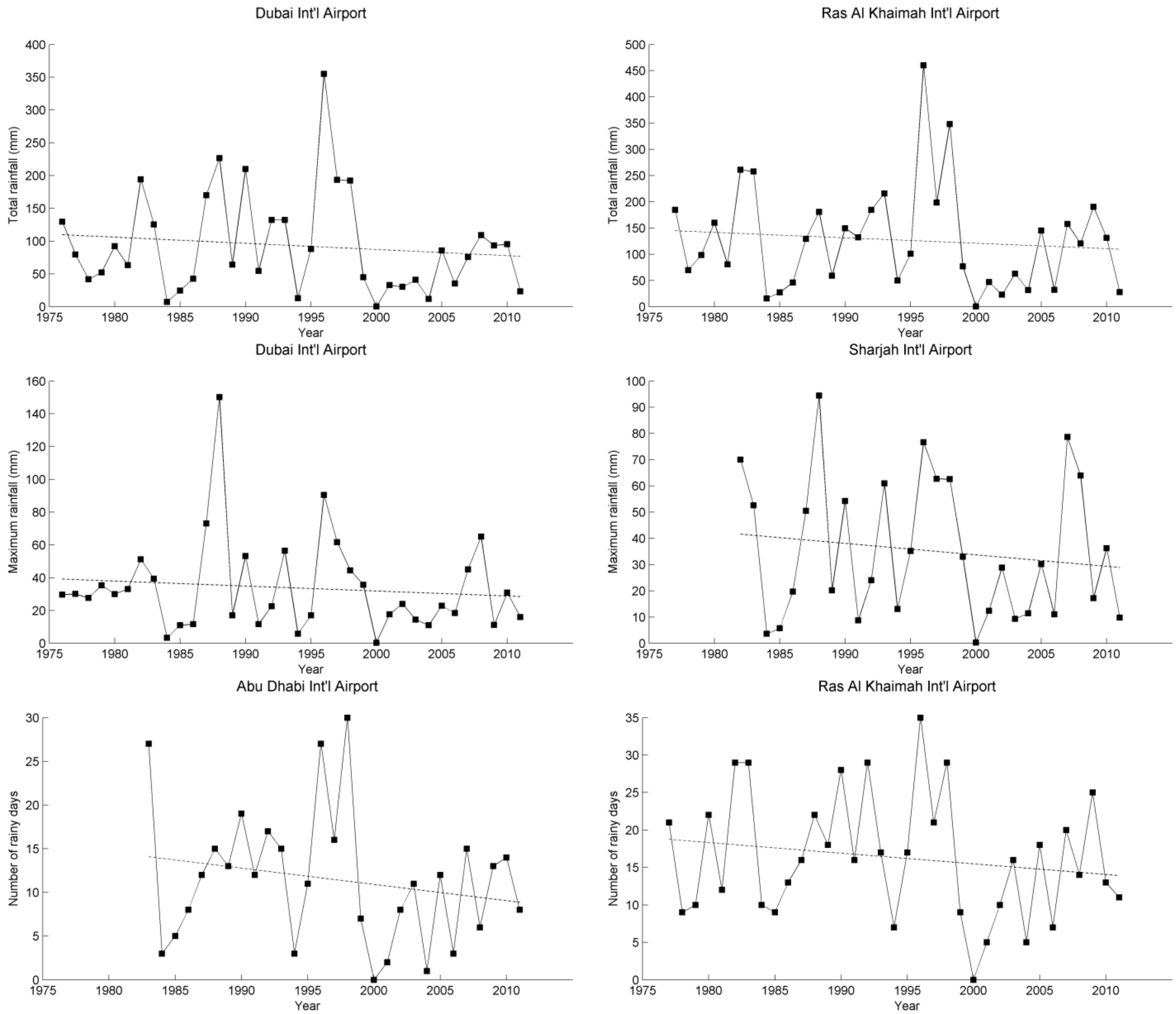

Dubai Int'l Airport
Total rainfall (mm)
Year
Ras Al Khaimah Int'l Airport
Total rainfall (mm)
Year
Dubai Int'l Airport
Maximum rainfall (mm)
Year
Sharjah Int'l Airport
Maximum rainfall (mm)
Year
Abu Dhabi Int'l Airport
Number of rainy days
Year
Ras Al Khaimah Int'l Airport
Number of rainy days
Year

Figure 4.

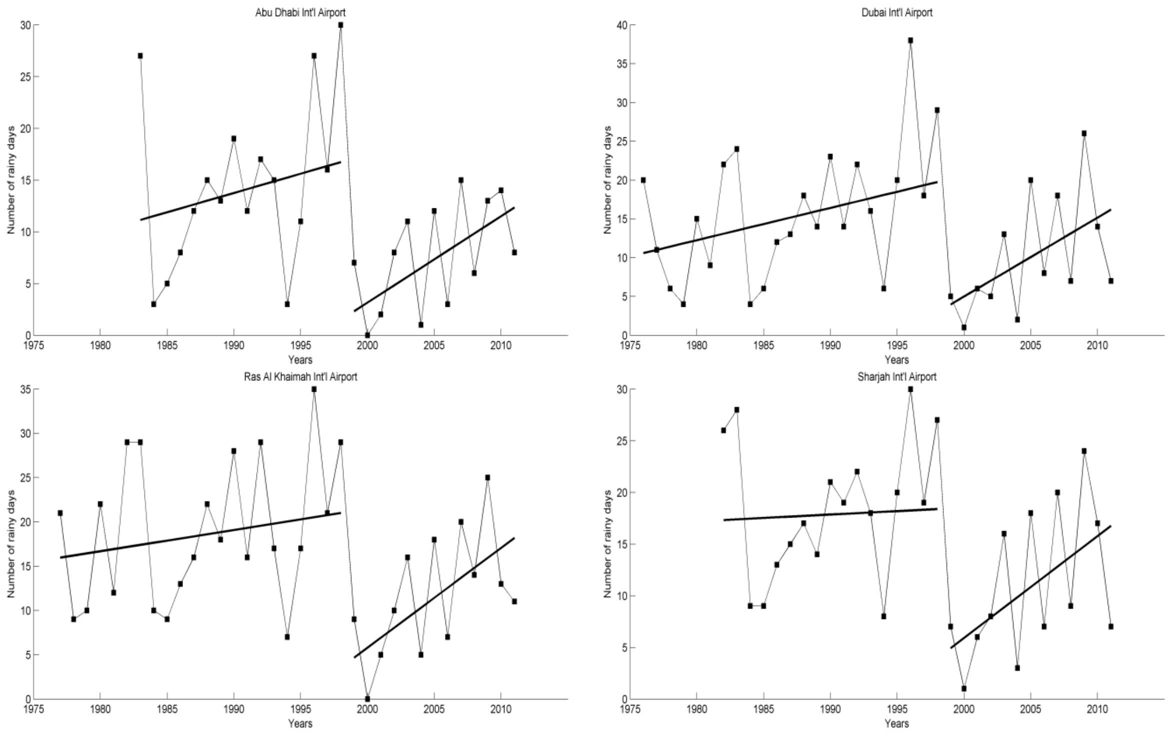
Abu Dhabi Int'l Airport
Dubai Int'l Airport
Ras Al Khaimah Int'l Airport
Sharjah Int'l Airport
Number of rainy days
Years

Figure 5.

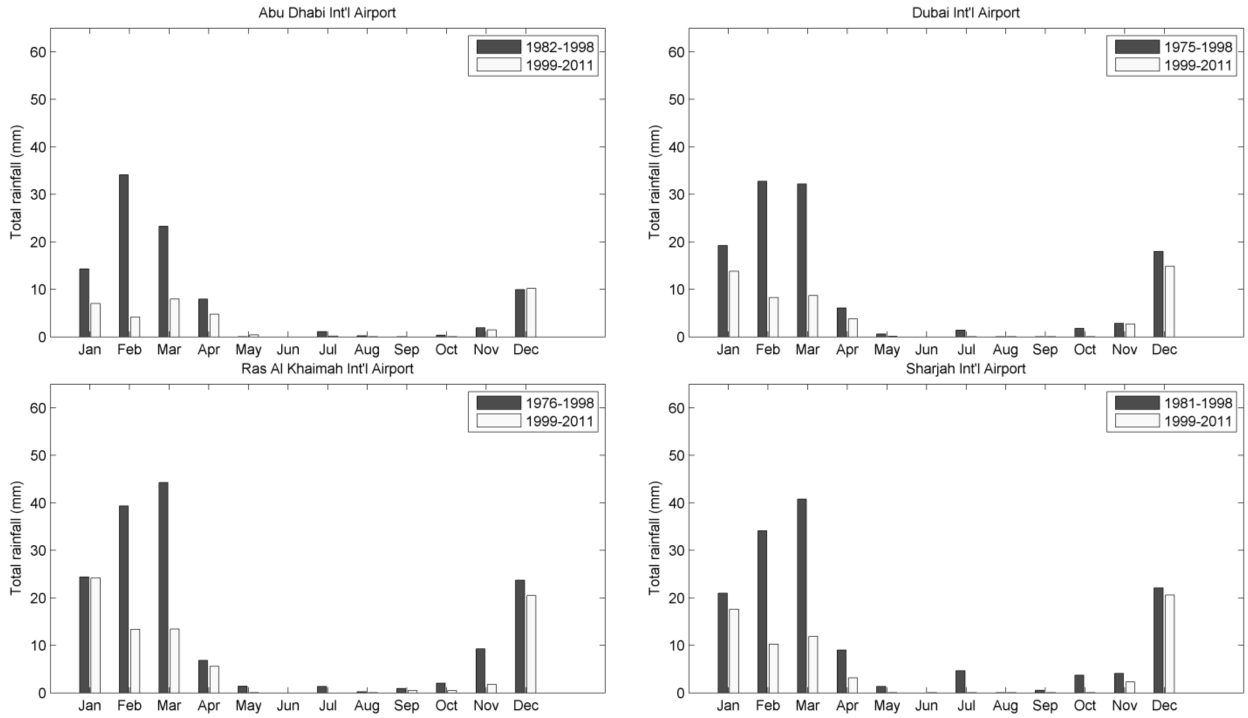
Abu Dhabi Int'l Airport
1982-1998
1999-2011
Dubai Int'l Airport
1975-1998
1999-2011
Ras Al Khaimah Int'l Airport
1976-1998
1999-2011
Sharjah Int'l Airport
1981-1998
1999-2011
Total rainfall (mm)
0
10
20
30
40
50
60
Jan
Feb
Mar
Apr
May
Jun
Jul
Aug
Sep
Oct
Nov
Dec
Figure 6.

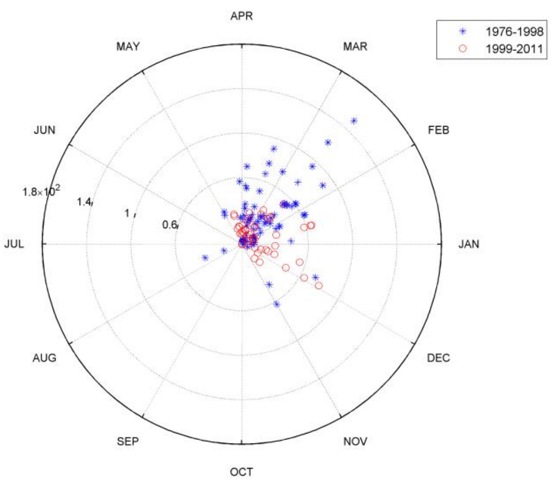
APR
MAR
FEB
JAN
DEC
NOV
OCT
SEP
AUG
JUL
JUN
MAY
1.8×10^2
1.4
1
0.6
1976-1998
1999-2011

Figure 7.

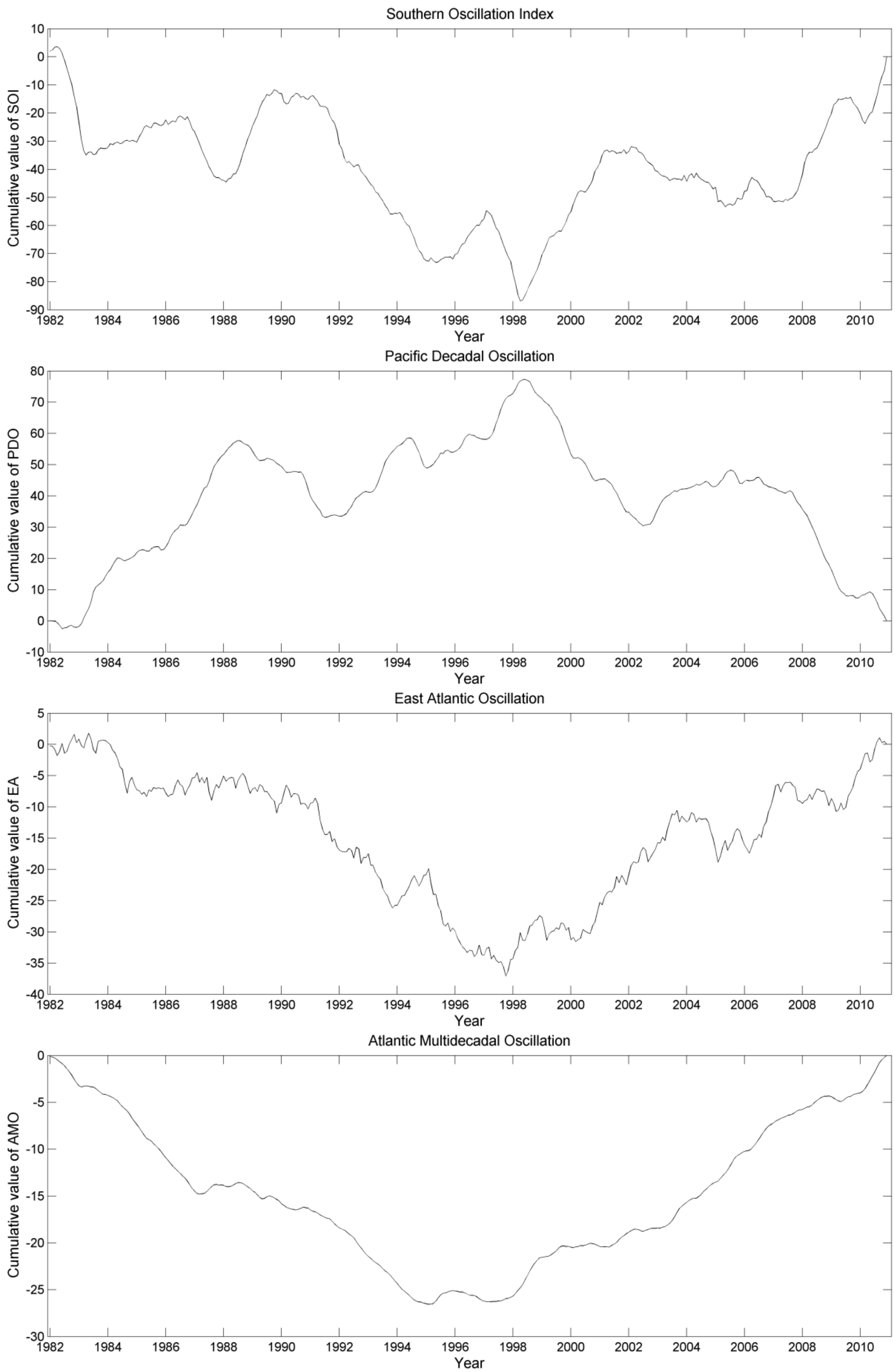
Southern Oscillation Index
Cumulative value of SOI
Year
Pacific Decadal Oscillation
Cumulative value of PDO
Year
East Atlantic Oscillation
Cumulative value of EA
Year
Atlantic Multidecadal Oscillation
Cumulative value of AMO
Year

Figure 8.

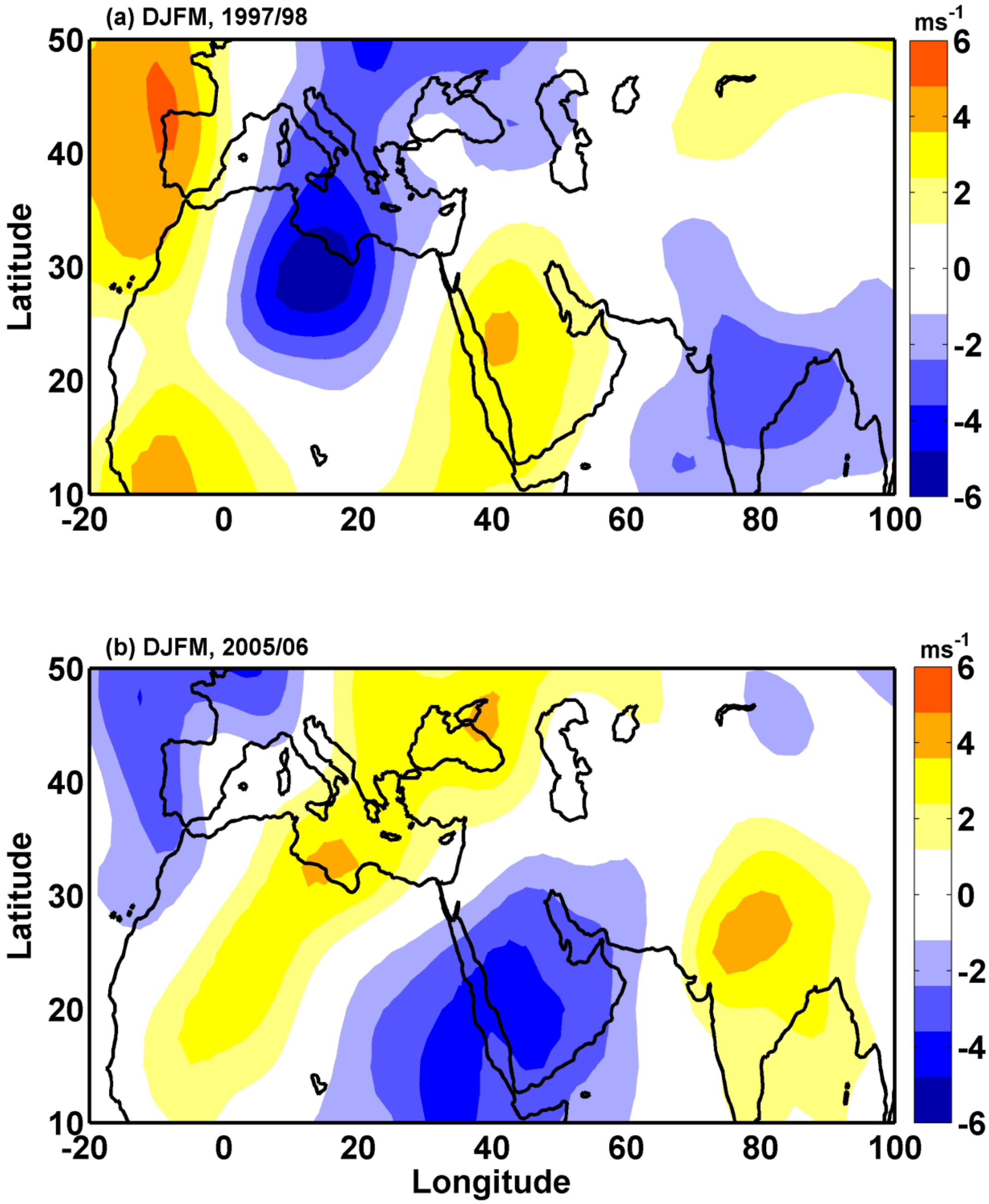

(a) DJFM, 1997/98
ms-1
6
4
2
0
-2
-4
-6
50
40
30
20
10
Latitude
-20
0
20
40
60
80
100
(b) DJFM, 2005/06
ms-1
6
4
2
0
-2
-4
-6
50
40
30
20
10
Latitude
-20
0
20
40
60
80
100
Longitude

Figure 9.

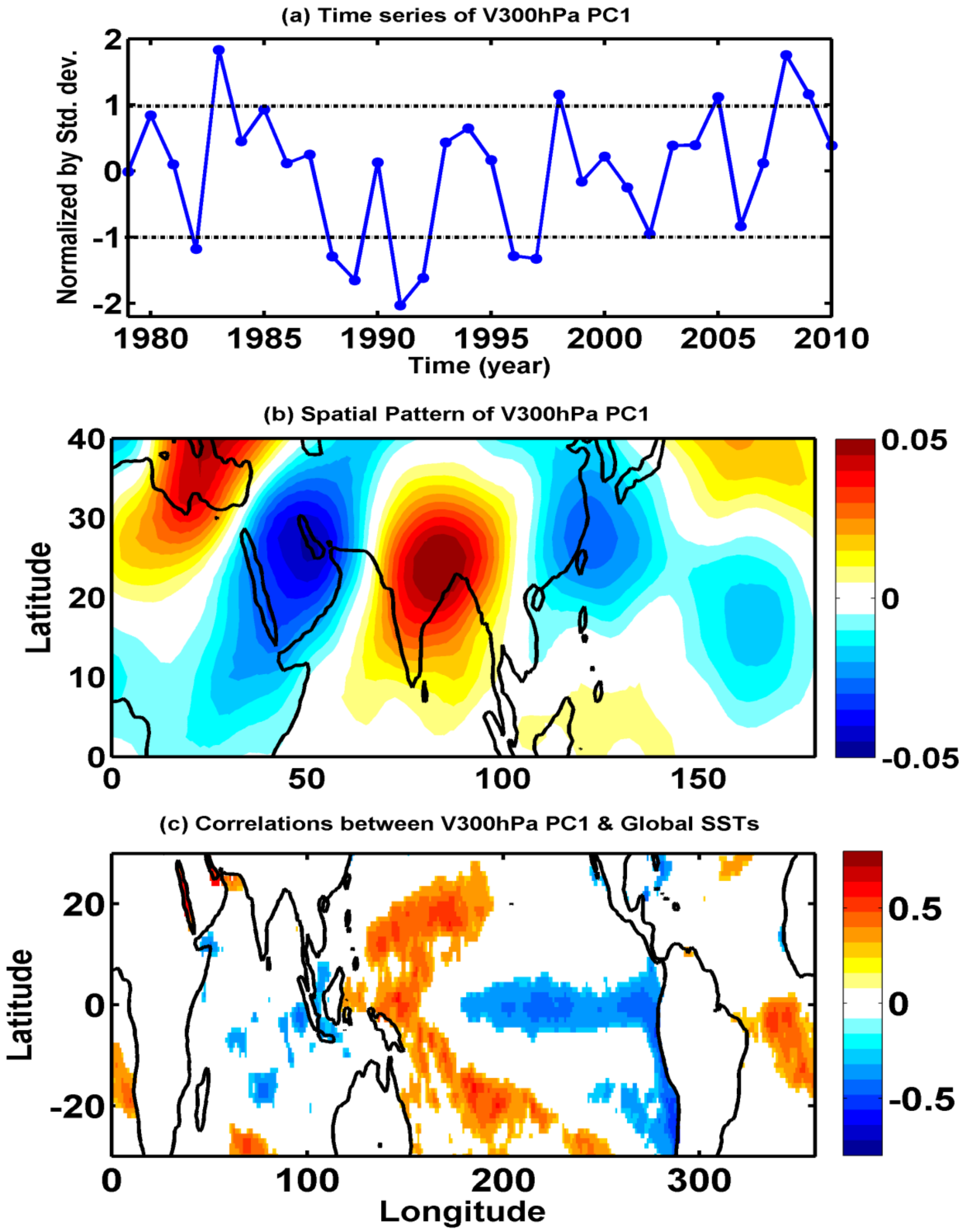

(a) Time series of V300hPa PC1
Normalized by Std. dev.
2
1
0
-1
-2
1980
1985
1990
1995
2000
2005
2010
Time (year)
(b) Spatial Pattern of V300hPa PC1
Latitude
40
30
20
10
0
0
50
100
150
0.05
0
-0.05
(c) Correlations between V300hPa PC1 & Global SSTs
Latitude
20
0
-20
0
100
200
300
Longitude
0.5
0
-0.5

Figure 10.